Increased Error Observability of an Inertial Pedestrian Navigation System by Rotating IMU

Khairi Abdulrahim[1], Chris Hide[2], Terry Moore[2] & Chris Hill[2]

[1]Facultyof Science and Technology, Universiti Sains Islam Malaysia (USIM),
Bandar Baru Nilai, Nilai 71800, Negeri Sembilan, Malaysia
[2]Nottingham Geospatial Institute, University of Nottingham,
NG7 2RD, Nottingham, UK
Email: khairiabdulrahim@usim.edu.my

Abstract. Indoor pedestrian navigation suffers from the unavailability of useful GNSS signals for navigation. Often a low-cost non-GNSS inertial sensor is used to navigate indoors. However, using only a low-cost inertial sensor for the system degrades its performance due to the low observability of errors affecting such low-cost sensors. Of particular concern is the heading drift error, caused primarily by the unobservability of z-axis gyro bias errors, which results in a huge positioning error when navigating for more than a few seconds. In this paper, the observability of this error is increased by proposing a method of rotating the inertial sensor on its y-axis. The results from a field trial for the proposed innovative method are presented. The method was performed by rotating the sensor mechanically–mounted on a shoe–on a single axis. The method was shown to increase the observability of z-axis gyro bias errors of a low-cost sensor. This is very significant because no other integrated measurements from other sensors are required to increase error observability. This should potentially be very useful for autonomous low-cost inertial pedestrian navigation systems that require a long period of navigation time.

Keywords: *error observability; inertial; low-cost; pedestrian navigation; sensor.*

1 Introduction

In indoor pedestrian navigation, where a reliable GNSS signal is often unavailable, the use of inertial sensors to navigate is not uncommon, see for example [1]. Although there are also alternative technologies for indoor navigation, such as WIFI-based, map-based, vision-based and magnetic-based solutions [2], the application of inertial sensors is more attractive because it is much cheaper in price compared to other technologies. Such navigation systems are widely known as inertial navigation systems (INS) and comprise an inertial sensor, commonly known as an inertial measurement unit (IMU), and a processor. Unlike GNSS, it uses the concept of dead reckoning, where the consecutive position and attitude relative to its initial position and initial attitude are computed from the IMU's acceleration and gyro data. Therefore an IMU is

Received, May 27th, 2013, Revised January 23rd, 2014, Accepted for publication May 7th, 2014.
 ISSN: 2337-5779, DOI: 10.5614/j.eng.technol.sci.2014.46.2.7

often used whenever the GNSS signal is compromised, because it does not require external signals for positioning and navigation.

However, the use of such a low-cost sensor for navigation comes with a cost, because of the concept of dead reckoning it uses and because it is an autonomous sensor, it needs to be initialized to some initial values before it can be fully used. Therefore, the initial position, velocity and attitude of the inertial sensor have to be obtained from external measurements, which sometimes is not convenient and can be problematic when indoors. However, for the purpose of this paper, this problem is assumed to be harmless because the assumption can be made that, for example before going indoors, there are at least some good estimations of position and attitude available from the use of GNSS outdoors. This information can provide the initial values that are needed to initialize the inertial sensors when indoors.

The focus of this paper is therefore on the remaining unobservable gyro error on the z-axis of the inertial sensor that causes the heading drift problem affecting low-cost pedestrian navigation systems (PNS), which may prove costly if it is not being handled carefully [3]. For a shoe-mounted low-cost PNS, the frequent use of Zero Velocity Update (ZUPT) measurements consistently bounds many of the IMU errors [4]. However, heading drift still remains despite the use of ZUPT because it is not possible to estimate the heading error using only these measurements. In this situation, we say that the heading error is unobservable. Observability is defined as the ability to determine an estimation from a given sequence of measurements. In this paper, an innovative approach to mitigate heading drift by improving the observability of z-axis gyro bias errors is proposed for a low-cost PNS by a rotating inertial measurement unit (RIMU) that is mounted on a shoe (or foot).

This paper is structured as follows. Section 2 introduces the concept of a low-cost PNS using a shoe-mounted RIMU. Next, Section 3 presents the mathematical equations describing the INS output after undergoing rotations because of the RIMU. Section 4 and 5 describes afield trial and its results. Finally, the paper is concluded in Section 6.

2 The Concept of a Shoe-Mounted RIMU

The concept is depicted in Figure 1. The low-cost IMU was mounted on a platform that rotated on a single axis, whilst the platform was attached to a pedestrian's shoe. The principle behind it is that if it were possible to physically 'flip' the IMU at regular intervals about a certain axis (suppose y-axis) such that the other axes (suppose x-axis and z-axis) are 'flipped', errors on the x- and z-

axes would be cancelled out, as these errors would have a positive and negative effect along the path every time the IMU is flipped.

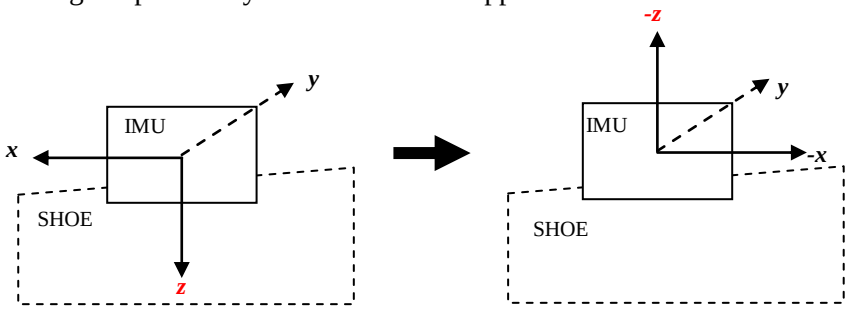

Figure 1 The concept of the RIMU for a low-cost PNS.

The concept of a rotating IMU to reduce IMU errors was introduced by Geller [5], in which he describes and computes the mathematical equations relating to the gyro rotating around its azimuth axis. Two terminologies were proposed in [6] for this concept: *carouselling* and *indexing*. The former was defined as rotating the IMU with continuous rotation in multiple orientations, while the latter was defined as rotating the IMU with discrete known rotation. Numerous other researchers also explored the same idea [7]-[17]. For clarity, however, the differences of all these approaches with the work in this paper are summarized below. This paper emphasizes:

1. Pedestrian navigation application with a low-cost IMU;
2. Performed in a real environment with a true walking trajectory;
3. Rotating the IMU on a single axis (y-axis) continuously throughout the trajectory; and
4. Neither carouselling–because of the single rotation axis–nor indexing was applied, because of the ambiguity of the rotation rate to the user.

Hence, the idea was adopted for a low-cost PNS as presented in this paper. Whilst this may be undesirable in terms of increasing the size, power and weight requirements of the IMU, it is not unrealistic to do so considering the exceptionally small mass of low-cost inertial sensors. Furthermore, the reliability and precision requirements for the mechanical parts are relatively low when considering a simple one-axis rotation, and there is no requirement for a constant or measurable rotation, since position–not rotation–is the output of concern.

3 Mathematical Analysis of RIMU

This section describes the effect of the RIMU on the estimated INS solutions of the low-cost PNS through error modulation, which subsequently increases the observability of error states. The Kalman Filter (KF) was used for the estimation process. The INS output resulting from the RIMU will be concisely analyzed by presenting a series of INS error equations.

3.1 INS Error Modulation

Velocity error states and attitude error states can be propagated using a standard strap down error navigation equation with a phi-angle error model [18]:

$$\delta\dot{\boldsymbol{v}}^n = \boldsymbol{C}_b^n\delta\boldsymbol{f}^b + \boldsymbol{C}_b^n\boldsymbol{f}^b \times \epsilon - (2\boldsymbol{\omega}_{ie}^n + \boldsymbol{\omega}_{en}^n) \times \delta\boldsymbol{v}^n - (2\delta\boldsymbol{\omega}_{ie}^n + \delta\boldsymbol{\omega}_{en}^n) \times \boldsymbol{v}^n + \delta\boldsymbol{g}^n \tag{1}$$

$$\dot{\epsilon} = -\boldsymbol{\omega}_{in}^n \times \epsilon + \delta\boldsymbol{\omega}_{in}^n - \boldsymbol{C}_b^n\delta\boldsymbol{\omega}_{ib}^b \tag{2}$$

In these two equations, $\delta\boldsymbol{\omega}_{ib}^b$ and $\delta\boldsymbol{f}^b$ are errors caused by gyroscope and accelerometer sensor errors. When the IMU is rotated about its y-axis, $\boldsymbol{C}_b^n$ is made to change continuously. Therefore, multiplication of $\delta\boldsymbol{\omega}_{ib}^b$, $\delta\boldsymbol{f}^b$ and $\boldsymbol{C}_b^n$ in the equations affects the navigation accuracy of the INS. The idea of an RIMU therefore lies in the periodical change of the elements in $\boldsymbol{C}_b^n$ such that the average of $\boldsymbol{C}_b^n\delta\boldsymbol{\omega}_{ib}^b$ and $\boldsymbol{C}_b^n\delta\boldsymbol{f}^b$ approximates zero.

When the RIMU is rotated about its y-axis, the angular rate error and the specific force error can be represented as:

$$\begin{aligned}\boldsymbol{C}_b^n\delta\boldsymbol{\omega}_{ib}^b &= \begin{pmatrix}\cos\omega_r t & 0 & \sin\omega_r t\\ 0 & 1 & 0\\ -\sin\omega_r t & 0 & \cos\omega_r t\end{pmatrix}\begin{pmatrix}\varepsilon_x\\ \varepsilon_y\\ \varepsilon_z\end{pmatrix}\\ &= \begin{pmatrix}\varepsilon_x\cos(\omega_r t) + \varepsilon_z\sin(\omega_r t)\\ \varepsilon_y\\ -\varepsilon_x\sin(\omega_r t) + \varepsilon_z\cos(\omega_r t)\end{pmatrix}\\ \boldsymbol{C}_b^n\delta\boldsymbol{f}^b &= \begin{pmatrix}\cos\omega_r t & 0 & \sin\omega_r t\\ 0 & 1 & 0\\ -\sin\omega_r t & 0 & \cos\omega_r t\end{pmatrix}\begin{pmatrix}\Delta_x\\ \Delta_y\\ \Delta_z\end{pmatrix}\end{aligned} \tag{3}$$

$$= \begin{pmatrix} \Delta_x \cos(\omega_r t) + \Delta_z \sin(\omega_r t) \\ \Delta_y \\ -\Delta_x \sin(\omega_r t) + \Delta_z \cos(\omega_r t) \end{pmatrix} \quad (4)$$

where ω_r is the RIMU rotation rate,$(\varepsilon_x \quad \varepsilon_y \quad \varepsilon_z)^T$ are the errors of the gyro on the x-, y- and z-axis, and, $(\Delta_x \quad \Delta_y \quad \Delta_z)^T$are the errors of the accelerometer on the x-, y- and z- axis.

From Eqs. (3) and (4), it follows that the IMU error terms for the x-axis and z-axis vary periodically due to the cosine and sine functions. This, however, is not the case for the y-axis because it is the rotation axis and does not have cosine and sine functions. If the x- and z-axis errors are constantly positive or negative over the whole rotation, the errors will then reduce to zero after a whole rotation period of $(60^0/\omega_r)$. The RIMU is therefore very effective in eliminating constant error terms on the IMU axes that are perpendicular with the rotation axis.

3.2 INS Error Observability

The principle of the RIMU in improving the error state observability of the INS can be explained by assuming the simple case of a stationary and level IMU. The velocity error model from Eq. (1) can be rewritten as [19]:

$$\delta \dot{\boldsymbol{v}}^n = \boldsymbol{C}_b^n \delta \boldsymbol{f}^b + \boldsymbol{C}_b^n \boldsymbol{f}^b \times \epsilon \quad (5)$$

The other terms in Eq. (1), containing the Earth's rotation and the gravity error, can be ignored since low-cost IMUs are not capable of measuring the Earth's rotation and also navigation is done with a low velocity in a small area (thus the gravity error is assumed insignificant). It can be written in a matrix form as:

$$\begin{pmatrix} \delta \dot{\boldsymbol{v}}_N \\ \delta \dot{\boldsymbol{v}}_E \\ \delta \dot{\boldsymbol{v}}_D \end{pmatrix} = \begin{pmatrix} 0 & -\boldsymbol{f}_D & \boldsymbol{f}_E \\ \boldsymbol{f}_D & 0 & -\boldsymbol{f}_N \\ -\boldsymbol{f}_E & \boldsymbol{f}_N & 0 \end{pmatrix} \begin{pmatrix} \epsilon_N \\ \epsilon_E \\ \epsilon_D \end{pmatrix} + \boldsymbol{C}_b^n \begin{pmatrix} \delta \boldsymbol{f}_x \\ \delta \boldsymbol{f}_y \\ \delta \boldsymbol{f}_z \end{pmatrix} \quad (6)$$

When the IMU is stationary and level, Eq. (6) becomes:

$$\begin{pmatrix} \delta \dot{\boldsymbol{v}}_N \\ \delta \dot{\boldsymbol{v}}_E \\ \delta \dot{\boldsymbol{v}}_D \end{pmatrix} = \begin{pmatrix} 0 & \boldsymbol{g} & 0 \\ -\boldsymbol{g} & 0 & 0 \\ 0 & 0 & 0 \end{pmatrix} \begin{pmatrix} \epsilon_N \\ \epsilon_E \\ \epsilon_D \end{pmatrix} + \begin{pmatrix} \delta \boldsymbol{f}_x & 0 & 0 \\ 0 & \delta \boldsymbol{f}_y & 0 \\ 0 & 0 & \delta \boldsymbol{f}_z \end{pmatrix} \quad (7)$$

where $\boldsymbol{C}_b^n$ is an identity matrix because of the small angle error approximation when stationary and level. When the IMU rotates 180degrees about its y-axis (still in a stationary and level mode), the $\boldsymbol{C}_b^n$ changes sign. Eq. (7) then becomes:

$$\begin{pmatrix} \delta\dot{\boldsymbol{v}}_N \\ \delta\dot{\boldsymbol{v}}_E \\ \delta\dot{\boldsymbol{v}}_D \end{pmatrix} = \begin{pmatrix} 0 & \boldsymbol{g} & 0 \\ -\boldsymbol{g} & 0 & 0 \\ 0 & 0 & 0 \end{pmatrix} \begin{pmatrix} \epsilon_N \\ \epsilon_E \\ \epsilon_D \end{pmatrix} + \begin{pmatrix} -1 & 0 & 0 \\ 0 & 1 & 0 \\ 0 & 0 & -1 \end{pmatrix} \begin{pmatrix} \delta\boldsymbol{f}_x & 0 & 0 \\ 0 & \delta\boldsymbol{f}_y & 0 \\ 0 & 0 & \delta\boldsymbol{f}_z \end{pmatrix} \quad (8)$$

Eqs. (7) and (8) can be written as simultaneous Eqs. (9) and (10):

$$\delta\dot{\boldsymbol{v}}_N = (+\boldsymbol{g})\epsilon_E + \delta\boldsymbol{f}_x \quad (9a)$$

$$\delta\dot{\boldsymbol{v}}_E = (-\boldsymbol{g})\epsilon_N + \delta\boldsymbol{f}_y \quad (9b)$$

$$\delta\dot{\boldsymbol{v}}_D = \delta\boldsymbol{f}_z \quad (9c)$$

$$\delta\dot{\boldsymbol{v}}_N = (+\boldsymbol{g})\epsilon_E - \delta\boldsymbol{f}_x \quad (10a)$$

$$\delta\dot{\boldsymbol{v}}_E = (-\boldsymbol{g})\epsilon_N + \delta\boldsymbol{f}_y \quad (10b)$$

$$\delta\dot{\boldsymbol{v}}_D = -\delta\boldsymbol{f}_z \quad (10c)$$

Eq. (9) shows when the RIMU is in a stationary and level condition, whilst Eq. (10) shows when the RIMU has rotated 180degrees about its *y*-axis (upside down). Eqs. (9a) & (10a) and (9c) & (10c) can then be solved simultaneously to observe accelerometer errors in the x- and z-axis through velocity error updates. The accelerometer error in the y-axis, however, cannot be made observable by the same Eqs. (9b) & (10b), since it is the rotation axis for the RIMU.

As for attitude errors, North and East attitude errors are observable through the velocity error updates because there is a large force in the Down axis resulting from the gravity heading when stationary (for example see Eq. (7)). The RIMU effect is therefore more appealing for making the attitude error in the Down axis more observable, where the error is not observable for a normal IMU when stationary. As in the previous discussion, the attitude error model for a low-cost IMU can be rewritten as (ignoring other terms because of the low-cost IMU used):

$$\dot{\epsilon} \quad = -\boldsymbol{C}_b^n \delta\boldsymbol{\omega}_{ib}^b \quad (11)$$

Again when stationary and level, Eq. (11) becomes:

$$\begin{pmatrix} \dot{\epsilon_N} \\ \dot{\epsilon_E} \\ \dot{\epsilon_D} \end{pmatrix} = \begin{pmatrix} 1 & 0 & 0 \\ 0 & 1 & 0 \\ 0 & 0 & 0 \end{pmatrix} \begin{pmatrix} \delta\boldsymbol{\omega}_x \\ \delta\boldsymbol{\omega}_y \\ \delta\boldsymbol{\omega}_z \end{pmatrix} \quad (12)$$

When the IMU rotates 90degrees about its *y*-axis, the$\boldsymbol{C}_b^n$ changes and Eq. (12) becomes:

$$\begin{pmatrix} \dot{\epsilon_N} \\ \dot{\epsilon_E} \\ \dot{\epsilon_D} \end{pmatrix} = -\begin{pmatrix} 0 & 0 & -1 \\ 0 & 1 & 0 \\ 1 & 0 & 0 \end{pmatrix} \begin{pmatrix} \delta\boldsymbol{\omega}_x \\ \delta\boldsymbol{\omega}_y \\ \delta\boldsymbol{\omega}_z \end{pmatrix} \tag{13}$$

Eq. (13) shows that the gyro sensor error on the z-axis is now made observable through the North attitude error. Because North attitude errors are already observable from Eq. (7), the correlated gyro sensor error on the z-axis (i.e. *z*-axis gyro bias) can therefore be observed as well.

Note that the discussion assumes the simple case of an IMU where it is stationary and level. Nevertheless, it does explain the principle of rotating the IMU for improving the observability of error states. In reality, however, many terms during the modelling and estimation process in the Kalman Filter (KF) may contain errors. For example, $\boldsymbol{C}_b^n$ and $(\boldsymbol{f}^n \times)$ may contain errors and the state transition matrix in the KF may not correctly model the propagation of errors. Nevertheless, by also improving the observability of error states, more information is updated in the KF. This will help during the estimation process, since these errors may correlate with other error states. Therefore, over time the KF can propagate more information about the uncertainty of all error states for a better estimation of the errors of the system.

4 RIMU Field Trial

This section presents the RIMU walking field trial. This was performed to identify the impact of the RIMU on the observability of IMU errors for a low-cost pedestrian navigation system. Results showing the estimated biases are presented afterwards.

The field trial was performed using the RIMU prototype shown in Figure 2, developed by the Geospatial Research Centre New Zealand (GRCNZ). Marker 'A' in Figure 2 (left) shows the platform that was designed to rotate and onto which an IMU was mounted. The IMU was 'strapped' onto the platform using a tape as rigid as possible, so that the IMU represented the actual motion of the platform. The IMU used was from MicroStrain (3DM-GX3-25), which was powered by a 12V battery carried in a backpack along with the data logger to log the raw IMU data. This should be a reasonable representation of a low-cost sensor, with technical specifications typical for a low-cost IMU grade with 44mm x 25 mm x 11 mm dimensions and weighing only 11.5g. The accelerometer bias stability is quoted as ±0.01 g, and for the 300°/s model, the gyro biases are specified as ± 0.2°/s. The particular IMU used had a limit of 1200°/s for angular rotation and 18g for acceleration. The black box marked 'B' in Figure 2 (right) is the RIMU controller and houses two 9V batteries. The platform rotation speed can be increased or decreased with a switch at the side

of the controller, although the exact rotation rate is unknown. There is also an ON/OFF switch on the controller to switch on or off the RIMU mode.

Figure 2 RIMU prototype with (left) IMU mounted on a rotating platform, and (right) the RIMU controller.

4.1 Trial Description

The rotation of the IMU platform was started from the beginning (upon powering on the device). A user equipped with the RIMU stood at the starting position so that the IMU's horizontal alignment could be made for approximately 1 *s* at the beginning of the walk. The user then performed two walks (back to back) around the Nottingham Geospatial Building (NGB) office area to create a rectangular trajectory around the office where the start and the end trajectory was the same, marked by a tape.

The first walk with the RIMU was for 10 rounds. At the end of the 10^{th} round, the RIMU mode was turned off by stopping the platform's rotation using the switch, whilst keeping the IMU switched on. The user walked again immediately for a second walk of another 10 rounds over approximately the same trajectory (by following straight features on the floor carpet). The two trials lasted for about 650 *s* each. The reference for comparison of error estimation was created based on the second walk, in which a method developed by the authors [20,21] was applied. The data were processed and analyzed in a Kalman Filter (KF) environment using the POINT software [22]. The error states modelled were the same as in [20,21] and are therefore not shown here.

4.1.1 Analysis Assumptions

Before an IMU error comparison between the two walks could be made, it is worthwhile to highlight that the impact of, for example, a temperature-dependent bias or a turn-on bias of the IMU is considered less destructive. This is because the two walks were performed back to back without switching the IMU off. The sensitivity of *a priori* process noise initial covariance and

measurement noise towards filter convergence [23] was also not considered. Both process noise and measurement noise were, therefore, given the same information to reduce the dependence of process convergence on the initial covariance.

Take note that it is actually impossible to quantify the true IMU errors for use as a reference for the trials, because they are unknown. For comparison purposes, implementing the method from [21] should give sufficient information about the best estimate of the IMU errors, because it gives a more accurate position solution. This, however, is slightly overoptimistic because in reality there will always be errors resulting from the inaccuracy when modelling the INS error propagation. The error in forces measured by the IMU will affect the estimation of the IMU attitude errors. This subsequently will affect the estimation of the IMU accelerometer errors because of the correlation between the error states. Therefore, it is assumed that the estimation of the accelerometer biases and gyro biases from [21] to be used as a reference are adequately estimated because of the high accuracy position solutions achieved. Although only a coarse comparison of IMU errors can be performed, this should give a general idea of the overall improvement made by the RIMU towards error observability.

The method from [21] was used as a reference to compare the bias estimation of the RIMU. Note that the IMU used for the reference was not rotated. This was done so that the actual improvement made by the RIMU to mitigate heading drift could be seen when the biases were made to be more observable. Two separate trials with the same trajectory were therefore performed: the actual trial with the RIMU and a reference trial without the RIMU (using the method from [21]).

Furthermore, a precise statistical analysis for the estimation of the IMU biases– for RIMU and reference trial (IMU + [21])–is deemed impossible because of the two following factors:

1. The two trials were not performed in exactly the same time, and
2. The reference trial was performed in a separate trial.

Unless both trials are completed in exactly the same period, the two factors will cause possible discrepancies when comparing the estimate of errors (for RIMU and non-RIMU) with the reference. The effect, however, is assumed to be negligible for analysis purposes.

5 Results

Figure 3 shows the z-axis gyro bias estimates for RIMU and non-RIMU, plotted against the reference. Both datasets were initialised with their average bias

values during alignment. It can be observed from the figure that RIMU has a similar plot to the reference, as opposed to non-RIMU. After about 50 *s*, RIMU has resolved and stabilized to within 0.05°/s from the reference, whilst non-RIMU has not resolved to the reference even at the end of the trial. This indicates that the z-axis gyro bias can be made observable through the use of RIMU as opposed to non-RIMU, where the z-axis gyro bias has converged to an incorrect value.

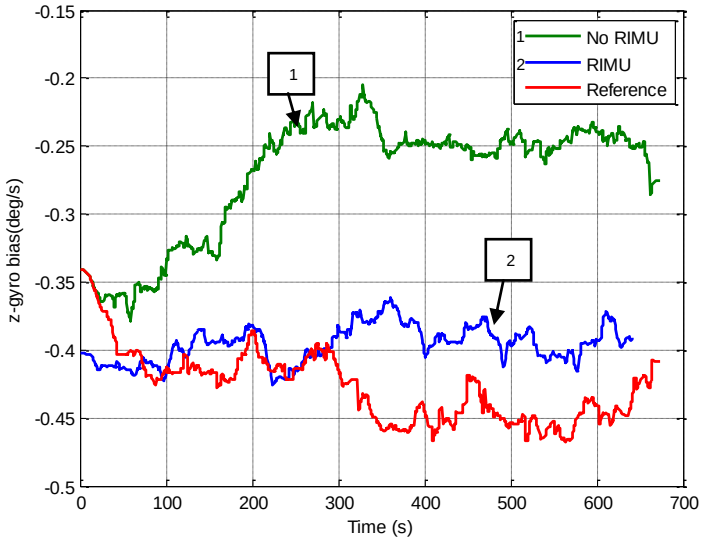

Figure 3 A comparison of z-gyro bias estimation with different approaches.

Figure 4 shows the x and y-axis gyro bias estimates for both RIMU and non-RIMU, plotted against the reference. Both x and y-axis gyro biases have been estimated to be well within 0.1°/s of the reference throughout the dataset. This indicates that the observability effect of the RIMU was not as influential as it was previously, when estimating the *z*-axis gyro bias. This is because both of these errors were observable using ZUPTs even when the IMU was not rotated. The velocity updates through ZUPTs, performed at every footstep during walking, had the effect of also estimating the correlated attitude errors on the *x*- and *y*-axis through Eq. (7).

The accelerometer biases on the *x*, *y* and *z*-axis for both RIMU and non-RIMU are plotted against the reference in Figure 5. It can be observed from the figure that implementing the RIMU in the walking trial had no significant advantage over non-RIMU when estimating the accelerometer biases for all three axes. With or without the RIMU, the accelerometer biases on the x, y and z-axes still resolved to within 0.05 $m/s^2$of the reference. This indicates that there is no

significant difference between the two cases (with or without RIMU) in the observability of all these errors. When walking, the accelerometer biases for both RIMU and non-RIMU were therefore well observed through ZUPTs because there were horizontal accelerations. For example, a forward acceleration can separate the pitch error and forward accelerometer bias (see Eq. (6)).

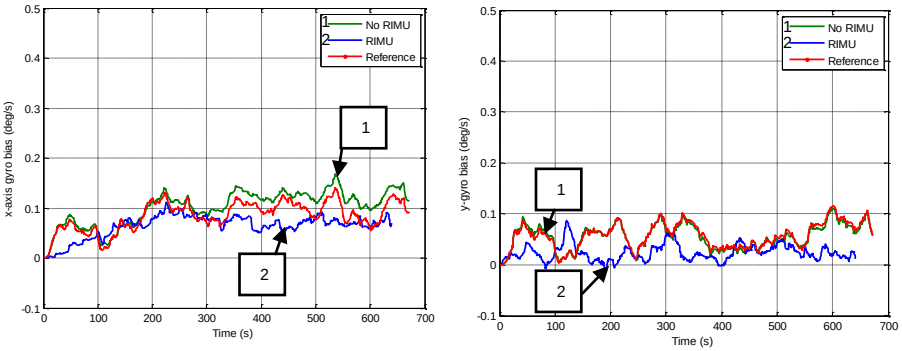

Figure 4 A comparison of (left) x-axis gyro bias, (right) y-axis gyro bias estimation with different approaches.

A closer look at Figure 5 shows there was a spike at the beginning of the dataset for the *x* and *z*-axis when the RIMU was implemented. This effect is observed for the *x* and *z*-axis accelerometer bias for the first 17 *s* of the dataset, when the RIMU remained stationary, with a maximum of 0.48 m/s^2 and 0.18 m/s^2 respectively. This was caused by the effect of having the RIMU rotate about its y-axis, which in turn caused the x- and z-axes to be rotated. As a result, the x- and z-axes displayed a certain amount of gravity acceleration during this rotation period. The higher uncertainty resulting from the higher initial process noise therefore gave too much weight from the innovation sequence to the bias estimates. However, as the KF received more information from the velocity updates, it was able to separate the attitude and acceleration errors. By setting a lower initial process noise, the spike at the beginning of the dataset was actually reduced, as shown in Figure 6. The proper initialization and estimation of the stochastic properties of the filter is a challenging task. Please refer, for example, to [23] and [24] for more details. Its discussion is beyond the scope of this paper because it concerns the convergence rates of the estimated states. This study only focused on the observability of error states (convergence to correct values) and therefore used a tuning approach for the KF [24].

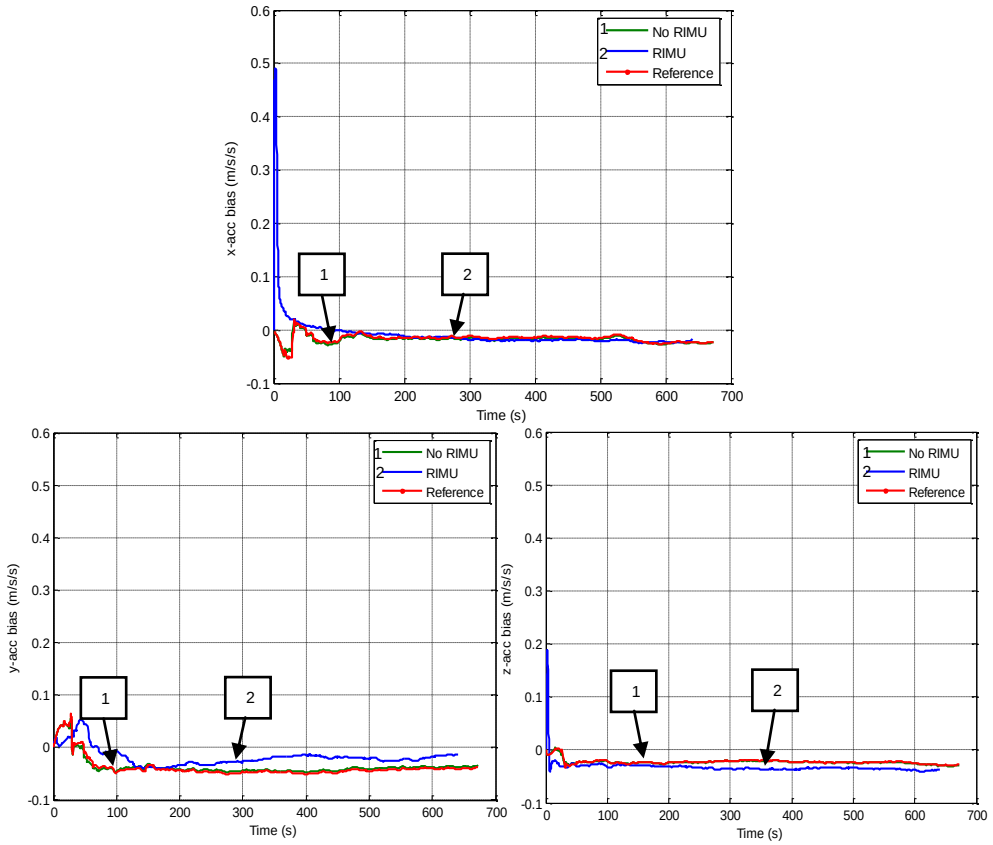

Figure 5 (Top to bottom, counter clockwise): x-, y- and z-accelerometer bias.

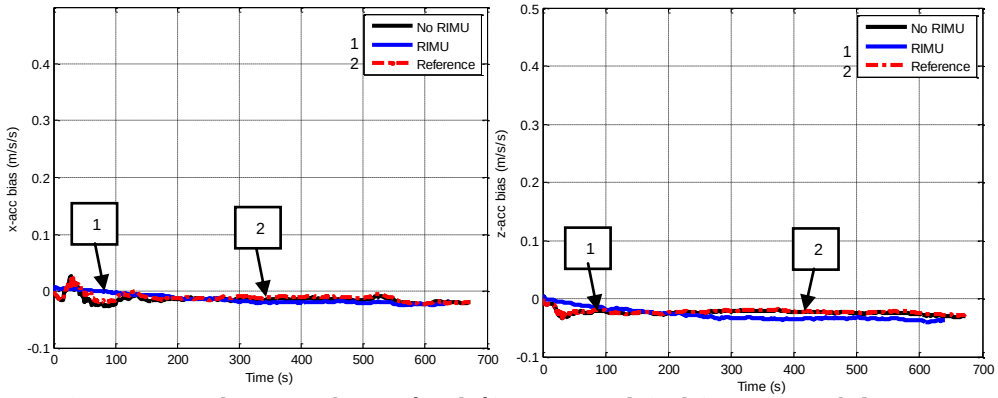

Figure 6 Accelerometer biases for (left) x-axis, and (right) y-axis, with lower initial process noise value.

6 Conclusion

A new approach of rotating an IMU (RIMU) for a low-cost PNS was presented. Through a field trial, it was shown to improve the observability of error states without the need of any other external measurements to feed the Kalman Filter (KF) apart from the available ZUPTs. Of particular interest was the z-axis gyro bias (which corrupted the INS heading) that is unobservable in a system that has no other external measurement update except ZUPTs. This error was thought to be the main error source contributing to the position drift, hence the significance of having a good estimation of this error, as presented in this paper.

It was shown that using the RIMU, the IMU error observability increased, particularly the z-axis gyro bias. This is a significant result towards having an autonomous inertial pedestrian navigation system because the remaining unobservable errors can now be made observable even without extra measurements to feed the KF. Nonetheless, more trials are worth performing to assess the RIMU's true capabilities once a better RIMU prototype is available. This is because the current RIMU prototype is too impractical for mass trials due to its weight and size. Once all components can be miniaturized, it will be more practical to attach them to a foot or shoe. Trials such as a real fire-fighter trial are thought to be useful to assess the RIMU's performance as it is supposed to better estimate (or observe) the error terms, regardless of the IMU bias variations that could be caused by, for example, extreme temperatures. Ultimately, this should further improve the navigation accuracy of an autonomous low-cost foot-mounted inertial navigation system.

Acknowledgments

The authors would like to thank the Universiti Sains Islam Malaysia (USIM) for partly sponsoring this study.

References

[1] Alvarez, J., Alvarez, D., López, A. & González, R.C., *Pedestrian Navigation Based on a Waist-Worn Inertial Sensor,* Sensors, **12**(8), pp. 10536-10549, 2012.

[2] Hui, L., Darabi, H., Banerjee, P., & Jing, L., *Survey of Wireless Indoor Positioning Techniques and Systems,* IEEE Transactions On Systems, Man & Cybernetics: Part C - Applications & Reviews, **37**(6), pp. 1067-1080, 2007.

[3] Jiménez, A.R., Seco, F.F., Zampella, F.F., Prieto, J.C. & Guevara, J.J. *Improved Heuristic Drift Elimination with Magnetically-Aided Dominant Directions (Mihde) for Pedestrian Navigation in Complex Buildings,* Journal of Location Based Services, **6(**3), pp. 186-210, 2012.

[4] Foxlin, E., *Pedestrian Tracking with Shoe-Mounted Inertial Sensors*, IEEE Computer Graphics & Applications, **25**(6), pp. 38-46, 2005.

[5] Geller, E.S., *Inertial System Platform Rotation*, IEEE Transactions on Aerospace and Electronic Systems, AES-4, pp. 557-568, 1968.

[6] Curey, R.K., Ash, M.E., Thielman, L.O. & Barker, C.H., *Proposed IEEE Inertial Systems Terminology Standard and Other Inertial Sensor Standards*. In Proceedings of Position, Location and Navigation Symposium (PLANS 2004), California, USA, 27-29 April 2004.

[7] Zha, F., Xu, J., Hu, B. & Qin, F., *Error Analysis for SINS with Different IMU Rotation Scheme*, In Proceedings of 2nd International Asia Conference on Informatics in Control, Automation and Robotics, Wuhan, China, 6-7 March 2010.

[8] Ben, Y.-Y., Chai, Y.-L., Gao, W. & Sun, F., *Analysis of Error for A Rotating Strapdown Inertial Navigation System with Fibro Gyro*, Journal of Marine Science and Application, **9**, pp. 419-424, 2010.

[9] An, L., Guo-bin, C., Fang-jun, Q. & Hong-wu, L., *Improved Precision of Strapdown Inertial Navigation System Brought by Dual-Axis Continuous Rotation of Inertial Measurement Unit*, in Proceedings of 2nd International Asia Conference on Informatics in Control, Automation and Robotics (CAR) 2010, Wuhan, China, 6-7 March 2010.

[10] Zhao, L., Wang, X.-Z., Huang, C. & Cheng, J.-H., *The Research on Rotation Self-Compensation Scheme of Strapdown Inertial System*, in Proceedings of the 2009 International Conference on Mechatronics and Automation (ICMA 2009), Jilin, China, 9-12 August 2009.

[11] Zhang, L., Lian, J., Wu, M. & Zheng, Z., *Research on Auto Compensation Technique of Strap-Down Inertial Navigation Systems*, in Proceedings of the International Asia Conference on Informatics in Control, Automation and Robotics, Bangkok, Thailand, 1-2 February 2009.

[12] Lai, Y.C., Jan, S. S. & Hsiao, F.B., *Development of A Low-Cost Attitude and Heading Reference System Using A Three-Axis Rotating Platform*, Sensors, **10**, pp. 2472-2491, 2010.

[13] Waldmann, J., *Feed Forwardings Aiding: An Investigation of Maneuvers for Inflight Alignment, Sba: Controle & Automação Sociedade*, Brasileira de Automatica, **18**, pp. 459-470, 2007.

[14] Syed, Z., Aggarwal, P., Goodall, C., Niu, X. & El-sheimy, N., *A New Multiposition Calibration Method for MEMS Inertial Navigation Systems*, Measurement Science and Technology, **18**, pp. 1897-1907, 2007.

[15] Ishibashi, S., Tsukioka, S., Yoshida, H., Hyakudome, T., Sawa, T., Tahara, J., Aoki, T. & Ishikawa, A., *Accuracy Improvement of an Inertial Navigation System Brought About by the Rotational Motion*, in

Proceedings of OCEANS 2007-Europe, Aberdeen, Scotland, 18-21 June 2007.

[16] Yang, Y. & Miao, L., *Fiber-Optic Strapdown Inertial System with Sensing Cluster Continuous Rotation*, *IEEE Transactions on Aerospace and Electronic Systems*, **40**, 1173, 2004.

[17] Qi, N., Xiaoying, G. & Zhun, L., *Research on Accuracy Improvement of INS with Continuous Rotation*, In Proceedings of the 2009 International Conference on Information and Automation (ICIA '09), Zuhai, China, 22-25 June, 2009.

[18] Klein, I., Filin, S., Toledo, T. & Rusnak, I., *Assessment of Aided-INS Performance*, Journal of Navigation, **65**(1), pp.169-185, 2012.

[19] Godha, S. & Lachapelle, G., *Foot Mounted Inertial System for Pedestrian Navigation*, Measurement Science and Technology, **19,** 075202, 2008.

[20] Abdulrahim, K., Hide, C., Moore, T. & Hill, C., *Aiding MEMS IMU with Building Heading for Indoor Pedestrian Navigation*, Proceeding of Ubiquitous Positioning Indoor Navigation and Location Based Service (UPINLBS), Helsinki, Finland, pp. 1-6, 2010.

[21] Abdulrahim, K., Hide, C., Moore, T., & Hill, C., *Aiding Low Cost Inertial Navigation with Building Heading for Pedestrian Navigation*, Journal of Navigation, **64**(2), pp. 219-233, 2011.

[22] Hide, C., *Algorithm Documentation for POINT Software*, Geospatial Research Centre, New Zealand, 2009.

[23] Hide, C., *Integration of GPS and Low Cost INS Measurements*, Ph.D. The University of Nottingham, United Kingdom, 2003.

[24] Groves, P.D., *Principles of GNSS, Inertial, and Multi-Sensor Integrated Navigation Systems*, Boston, United States: Artech House, 2008.